Electronic Structure and Bonding of $\{Fe(PhNO_2)\}^6$ Complexes: A Density Functional Theory Study

Olexandr Isayev,[†] Leonid Gorb,[†] Igor Zilberberg,[‡] and Jerzy Leszczynski*,[†]

Computational Center for Molecular Structure and Interactions, Jackson State University, Jackson, Mississippi 39217, and Boreskov Institute of Catalysis, Novosibirsk 630090, Russia

Received: October 19, 2006; In Final Form: January 31, 2007

Reduction of nitro-aromatic compounds (NACs) proceeds through intermediates with a partial electron transfer into the nitro group from a reducing agent. To estimate the extent of such a transfer and, therefore, the activity of various model ferrous-containing reductants toward NAC degradation, the unrestricted density functional theory (DFT) in the basis of paired Löwdin−Amos−Hall orbitals has been applied to complexes of nitrobenzene (NB) and model Fe(II) hydroxides including cationic $[FeOH]^+$, then neutral $Fe(OH)_2$, and finally anionic $[Fe(OH)_3]^-$. Electron transfer is considered to be a process of unpairing electrons (without the change of total spin projection S_z) that reveals itself in a substantial spin contamination of the unrestricted solution. The unrestricted orbitals are transformed into localized paired orbitals to determine the orbital channels for a particular electron-transfer state and the weights of idealized charge-transfer and covalent electron structures. This approach allows insight into the electronic structure and bonding of the $\{Fe(PhNO_2)\}^6$ unit (according to Enemark and Feltham notation) to be gained using model nitrobenzene complexes. The electronic structure of this unit can be expressed in terms of π-type covalent bonding $[Fe^{+2}(d^6, S = 2) - PhNO_2(S = 0)]$ or charge-transfer configuration $[Fe^{+3}(d^5, S = 5/2) - \{PhNO_2\}^- ((\pi^*)^1, S = 1/2)]$.

Introduction

Selective reduction of nitroaromatic compounds (NACs) by ferrous iron has relevance to many areas of basic science and technology. One application of this reaction is related to the synthesis of various industrial products such as antioxidants, insecticides, and photolacquers from nitrosobenzene.[1] Transition metals and particularly iron oxo-compounds are known to exhibit catalytic activity in this process.[2] Another application concerns the development of cleanup technologies for the disposal of nitroaromatics (NACs).[3] This presents a major challenge for environmental science. Such development involves the coordination of experimental and theoretical investigations in order to integrate both technological and fundamental aspects of key processes. The iron hydroxo-species are among the most attractive NAC-reducing agents, being extremely cheap and environmentally clean.

Traditionally, several different approaches have been utilized to gain direct or indirect electronic and geometric structural information about catalytic active sites: a macroscopic approach using wet chemistry data and surface complexation models,[4,5] a microscopic approach using scanning force microscopy (STM),[6] and various techniques of X-ray absorption spectroscopy (XAFS, EXAFS, PTRF-XAFS).[7,8] Although the major processes affecting the iron treatment of NACs have been investigated qualitatively,[9−11] many issues regarding the reaction mechanism remain unsolved. The numerous available experimental studies do not provide general conclusions about the relative importance of various ferrous iron species with respect to NAC transformations. Depending on the type of Fe(II) and the solution composition, in particular pH, the obtained transformation rates can vary by several orders of magnitude, and in some cases different transformation products may be found. To this end, new methods need to be developed that allow one to assess the reactivities of different ferrous iron species, particularly when present in complex natural systems.[12,13]

Following the progress of modern quantum chemistry and high-performance computing, theoretical calculations provide a reliable way to investigate the geometry of these complexes and to determine the most preferred binding site of neutral and ionic forms of Fe (II) compounds. In addition, theory can also shed light on the electronic structure and bonding of metal atom/ion on the nitrobenzene substrate. Such properties are mostly determined by the characteristics of the ferrous center and the immediately interacting groups. Therefore, by analogy with the very well-known $\{FeNO\}^7$ unit,[14,15] we can define our system of interest as being the $\{Fe(PhNO_2)\}^6$ unit according to the Enemark and Feltham notation.[16] The number "six" originates from the fact that only $3d^6$ iron electrons contribute to the unit, whereas nitrobenzene represents a close-shell group supplying no electrons.

As widely accepted[3,17] the reduction of NACs (as a rule to corresponding amino-group species) by various reducing agents proceeds through intermediates with a partial electron transfer from reductant into the nitro group. To estimate the extent of such a transfer and, therefore, the activity of various model ferrous-containing reductants toward NAC degradation density, the density functional theory (DFT) has been applied to study complexes of nitrobenzene (NB) and model Fe(II) hydroxides starting from cationic $[FeOH]^+$, then neutral $Fe(OH)_2$, and finally anionic $[Fe(OH)_3]^-$. The density functional theory has proven successful in determining equilibrium geometries and electronic properties in similar transition-metal systems where an atom or cation interacts with medium-size molecules.[18−24] We use DFT to optimize the geometries and evaluate the

* Corresponding author. E-mail: jerzy@ccmsi.us.
[†] Jackson State University.
[‡] Boreskov Institute of Catalysis.

10.1021/jp0668798 CCC: $37.00
Published on Web 04/19/2007

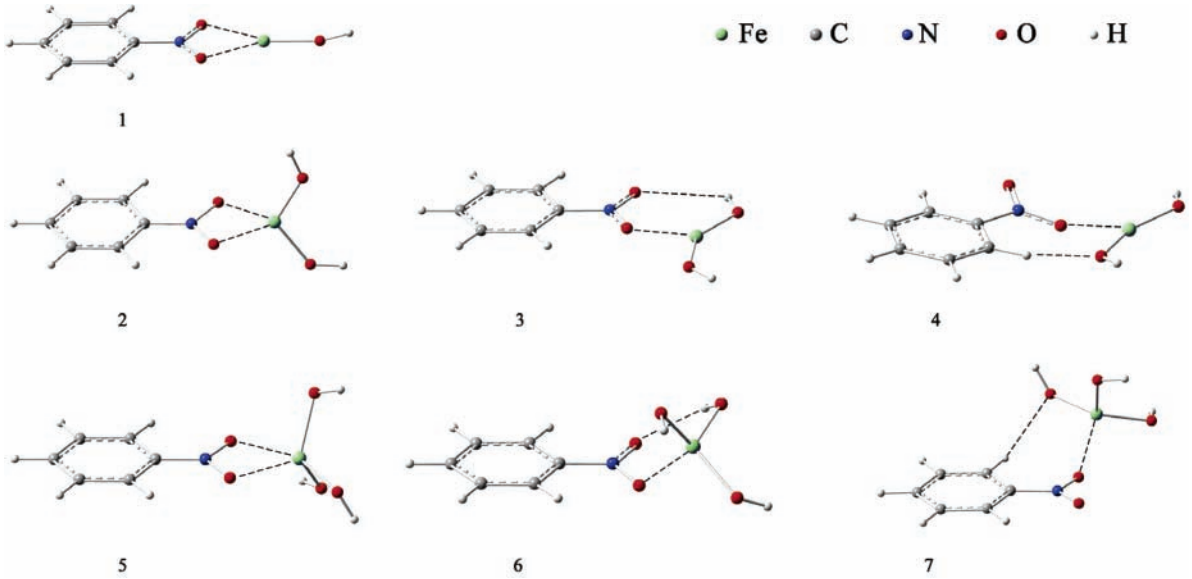

Figure 1. Structure of nitrobenzene−iron hydroxo complexes (**1**−**7**) obtained at the UB3LYP/6311+G(d) level.

electronic structure and binding of the ground (high spin) states of these complexes.

In the Methodology section, we briefly describe the applied computational procedure. The results are presented and discussed in the next section. Finally, we summarize our results in the Conclusions.

Methodology

The GAUSSIAN 03 package[25] was used for performing all calculations. The calculations using different spin states revealed that only those with spin projection $S_Z = 2$ need to be considered. Consequently, just these results are reported. All calculations were carried out within the unrestricted DFT using the hybrid three-parameter Becke's functional (B3LYP)[26] and, for comparison, the combination of Becke's exchange and LYP correlation gradient-corrected functionals (BLYP).[27,28] The standard 6-311++G(d) basis set was employed for light atoms along with the Wachters-Hay[29,30] all-electron basis set for iron (using the scaling factors of Raghavachari and Trucks[31]) supplemented by diffuse functions. The latter basis set for iron will be denoted as 6-311++G(d). It has been shown[32] that utilization of the triple-ξ basis set with polarization and diffusion function (6-311+G(d) in particular) is sufficient to reproduce the geometry of mononuclear non-heme iron centers, for example, Fe(EDTA)−NO. A natural bond orbital (NBO) analysis was performed by the standard protocol[33] as employed in GAUSSIAN 03. The visualization of orbitals has been performed by means of the MOLDEN program.[34] Obtained solutions for all of the complexes considered in the paper are available as Gaussian-formatted checkpoint files from the wavefunction database developed by NQMLab (www.nqmlab.com).

To identify the ground-state geometry (i.e., the most preferred Fe binding site on nitrobenzene), different starting configurations were considered in the geometry optimization procedure. These geometries were completely optimized without any symmetry constraints. The nature of the ground-state geometry was confirmed by computing the vibrational frequencies. Ground-state solutions were verified for internal instability. No BSSE correction for the interaction energies has been made.

To determine the orbital channels for electron transfer from the ferrous center into the nitro group, the electron transfer is considered as a process of unpairing electrons (initially set at the reductant) to form a couple of spin-up and spin-down electrons shared by the ferrous center and the nitro group. Such pairs of spatially separated, spin-up and spin-down orbitals are obtained in this work by transformation of unrestricted orbitals to a basis of paired (corresponding) Löwdin−Amos−Hall orbitals[35,36] where the space of paired orbitals (POs) is divided into subspaces of completely, partially, and non-overlapping orbitals. Paired orbitals along with the weights of various electron-transfer configurations contributing to a particular unrestricted DFT solution are obtained using the so-called S^2-expansion technique.[37] Spin contamination is shown to be associated with the "active" space of $2n$ partially overlapping POs. On the basis of POs, the unrestricted determinant is expanded in a linear combination of restricted determinants describing basis configurations contained 0,1, . . . , n pairs of spatially separated α and β spins.[37]

In considered species, nitro group coordinates via several sites with the iron center. Therefore, the coordinating atoms are identified using the IUPAC κ-notation. A superscripted number following the κ denotes the number of atoms of the ligand that are bound to the metal.

Results and Discussion

The optimized geometries of all considered species are depicted in Figure 1. The selected physical and geometrical parameters of **1**−**7** are presented in Table 1. Several types of nitro group coordination in the considered complexes have been found. κ^2 complexes (**1**, **2**, **5**) where iron is symmetrically coordinated with both oxygen atoms of nitro group, κ^1 (**3**, **4**, **6**, **7**) with side-on (**3**, **4**) and out-of-plate (**6**, **7**) orientation of iron center. In addition, there are two types of auxiliary hydrogen bonding found for the considered species. Either the hydrogen of the ferrous center is coordinated with the oxygen of the nitro group (**3**, **6**) or the hydrogen of the benzene ring is coordinated with oxygen next to iron. Despite the presence of some hydrogen bonding, the electronic structure of these complexes remains practically the same. Most probably, this is not an exhaustive list of all possible geometrical variations; however, a more extensive geometry search goes beyond the scope of present work.

For the NB...$[FeOH]^+$ system **1** we were unable to locate the κ^1 side-on complex. For $Fe(OH)_2$, the κ^2 symmetric complex

TABLE 1: Total Energy (E_{tot}, au), Relative (E_{rel}, kcal/mol) and Interaction Energy (ΔE, kcal/mol) along with Selected Geometrical Parameters as Obtained at the UB3LYP/6-311+G(d) and UBLYP/6-311+G(d) Levels for 1−7

system	method	E_{tot}	E_{rel}	ΔE	N−O	Fe···O	Fe−O(H)	∠O−N−O	∠N−O−Fe
1	BLYP	−1776.14886	0	−65.1	1.282	2.187	1.732	115.9	92.3
	B3LYP	−1776.22593	0	−84.2	1.257	2.192	1.730	116.4	92.6
2	BLYP	−1852.25584	0	−14.7	1.310	2.133	1.830	114.7	91.0
	B3LYP	−1852.34025	0	−31.4	1.310	2.051	1.808	113.0	91.3
3	BLYP	−1852.25504	0.5	−14.2	1.308; 1.256	2.005	1.824	121.9	126.0
	B3LYP	−1852.33847	1.1	−30.2	1.263; 1.230	2.046	1.816	122.8	129.9
4	BLYP	−1852.25237	2.2	−12.5	1.300; 1.247	1.987	1.839; 1.814	121.7	142.2
	B3LYP	−1852.33800	1.4	−29.9	1.244; 1.219	2.165	1.841; 1.809	122.6	155.5
5	BLYP	−1928.17936	6.1	−15.2	1.312	2.199	1.915[a]	114.9	92.3
	B3LYP	−1928.28236	4.6	−14.8	1.297	2.164	1.885[a]	115.4	92.4
6	BLYP	−1928.18913	0	−21.3	1.332; 1.298	2.063	1.898[a]	121.1	119.8
	B3LYP	−1928.28963	0	−19.4	1.321; 1.271	2.017	1.871[a]	121.1	122.1
7	BLYP	−1928.18797	0.7	−20.6	1.330; 1.281	2.034	1.904[a]	121.1	127.8
	B3LYP	−1928.28755	1.3	−18.1	1.329; 1,280	2.029	1.896[a]	121.0	128.2

[a] Averaged values.

TABLE 2: Mean Value of the S^2 Operator before ($\langle S^2\rangle$) and after Annihilation ($\langle S^2\rangle_A$) of the First Contaminant along with Mulliken Spin Densities as Obtained at the UBLYP/6-311+G(d) and UB3LYP/6-311+G(d) Levels

				Mulliken spin densities			
system	method	$\langle S^2\rangle$	$\langle S^2\rangle_A$	N	Fe	O(H)	O(N)
1	BLYP	6.010	6.000	0.05	3.59	0.35	0
	B3LYP	6.010	6.000	0.03	3.71	0.28	−0.01
2	BLYP	6.528	6.003	−0.17	3.82	0.31	−0.08
	B3LYP	6.882	6.022	−0.35	4.07	0.31	−0.08
3	BLYP	6.306	6.002	−0.14	3.76	0.28	0.05; −0.17
	B3LYP	6.184	6.001	−0.09	3.82	0.18	0.06; −0.13
4	BLYP	6.176	6.001	−0.08	3.68	0.23, 0.25	0.02; 0.08
	B3LYP	6.029	6.000	0.03	3.76	0.10, 0.14	0.04; 0.24
5	BLYP	6.831	6.008	−0.20	3.95	0.27	−0.15; −0.16
	B3LYP	6.966	6.022	−0.27	4.14	0.24	−0.16; −0.19
6	BLYP	6.636	6.006	−0.23	3.83	0.25 − 0.28	−0.01; −0.23
	B3LYP	6.891	6.018	−0.31	4.10	0.22 − 0.25	−0.01; −0.30
7	BLYP	6.688	6.006	−0.24	3.88	0.24 − 0.27	0.03; −0.27
	B3LYP	6.839	6.016	−0.31	4.07	0.21 − 0.23	0.04; −0.32

was found to be the global minima; the side-on complexes lie about 1−2 kcal/mol higher. This is consistent with other nitrobenzene-bivalent metal complexes, for example, NB−MgO.[38] In contrast, the side-on complexes NB...[Fe(OH)$_3$]$^-$ (**6**, **7**) are found to be ∼5 kcal/mol more stable than symmetric complex. Such behavior can be in principle described from an electrostatic point of view. Being positively charged, [FeOH]$^+$ strongly attracts negatively charged oxygens of the nitro group. These attractive forces highly stabilize the symmetric frontal orientation of [FeOH]$^+$ making the other minima extremely weak and flat. This is probably the reason that other orientations were unable to be located. On the contrary, the excess negative charge destabilizes the κ^2 complex orientation, pushing the components out. The destabilized minima **5** have been located for this case. The systematic decreasing of interaction energies ΔE calculated at the UB3LYP level in the group of **1**−**3**−**5** provides additional evidence supporting the discussion above. The results of the calculations predicted by UBLYP can be attributed to the fact that pure GGA functionals systematically underestimate the Fe−O binding energy (by 15−20 kcal/mol in some cases) compared to hybrid GGAs.[39,40]

Unrestricted solutions for the $S_Z = 2$ state of **2**,**5**,**6** reveal values of $\langle S^2\rangle$ exceeding their eigenvalues by about 0.9−1.0 and 0.5−0.8 at the B3LYP and BLYP levels, respectively. These states appear to be of the spin density wave (SDW) type[41] as seen from Mulliken spin densities for both pure and hybrid functionals (Table 2). Alternatively, the $\langle S^2\rangle$ values for **1** and **4** deviate only slightly from its eigenvalue of 6.0, indicating their almost pure quintet state. Annihilation of a septet contaminant from the $S_Z = 2$ state for all considered systems produces an almost pure quintet state, highlighting the septet's predominant contribution to the spin contamination. From this point of view, we can subdivide our model complexes into two groups: with significant spin contamination and without significant spin contamination. The first group corresponds to the appearance of spin densities on the nitro group of the nitrobenzene moiety.

To gain deeper insight into the effective electron configuration responsible for the $S_Z = 2$ unrestricted solution of the {Fe(PhNO$_2$)}^{6} unit, the corresponding Kohn−Sham determinant (Ψ_{KS}) has been expanded into a linear combination of restricted determinants constructed from "active" paired orbitals within the S^2 expansion technique developed in ref 37. This expansion was first successfully applied to the Fe(NO)(OH)$_2$ model system for the {FeNO}^{7} unit.[42] Active paired orbitals a_r and b_r, (and unoccupied a_r^v and b_r^v orbitals) correspond to pairs of natural orbitals with distinct occupancies between 2 and 0 (fully occupied and unoccupied, respectively) in magnitude. For example, compound **2** has a pair of orbitals with occupancies (1.692, 0.308) at the BLYP level and (1.378, 0.622) at the B3LYP level, respectively, that are really distinguishable from others. Those pairs will be referred to as orbitals (λ_1, μ_1) with occupancies (n_1, $2 - n_1$). The corresponding orbitals for other systems are marked in bold in Table 3; the shapes of all of these orbitals are represented in Figure 2. As was determined previously,[35] orbitals with occupancies close to two and singly occupied orbitals constitute an almost pure spin subsystem with $S = S_Z$ that makes negligible contribution to spin contamination.

TABLE 3: Integrals of Overlap $\langle a_1|b_1\rangle$ between a_1 and b_1 (See Figure 3) Responsible for Spin Contamination in $\{FePhNO_2\}$,[6] Occupancies of a_1 and a_1^v Orbitals, Weights of Restricted Determinants Appeared in the Expansion of KS Determinant for Active Parts and Occupancies of Natural Orbitals as Revealed by UBLYP/6-311+G(d) and UB3LYP/6-311+G(d) Level Calculations

					population		
system	method	$\langle a_1\|b_1\rangle$	a_1	a_1^v	D^0	D^1	natural orbital occupations
1	BLYP	0.998	1.998	0.998	99.17	0.83	2.000, 1.999, 1.998, 1.000, 1.000, 1.000, 1.000, 0.002, 0.001, 0.000
	B3LYP	0.998	1.998	0.998	99.34	0.66	2.000, 1.999, 1.998, 1.000, 1.000, 1.000, 1.000, 0.002, 0.001, 0.000
2	BLYP	0.692	1.692	0.308	47.83	52.17	2.000, 1.999, 1.999, **1.692**, 1.000, 1.000, 1.000, 1.000, **0.308**, 0.001, 0.001, 0.000
	B3LYP	0.378	1.378	0.622	14.28	85.72	2.000, 1.999, 1.999, 1.999, 1.999, 1.998, 1.996, **1.378**, 1.000, 1.000, 1.000, 1.000, **0.622**, 0.004, 0.002, 0.001, 0.001, 0.001, 0.000
3	BLYP	0.836	1.836	0.163	70.05	29.95	2.000, 1.999, **1.837**, 1.000, 1.000, 1.000, 1.000, **0.163**, 0.001, 0.000
	B3LYP	0.908	1.909	0.091	82.56	17.44	2.000, 1.999, 1.999, 1.998, 1.909, 1.000, 1.000, 1.000, 1.000, 0.091, 0.002, 0.001, 0.001, 0.000
4	BLYP	0.910	1.910	0.090	82.91	17.09	2.000, 1.999, **1.910,** 1.000, 1.000, 1.000, 1.000, **0.090**, 0.001, 0.000
	B3LYP	0.988	1.988	0.012	97.61	2.39	2.000, 1.999, 1.998, **1.988**, 1.000, 1.000, 1.000, 1.000, **0.012**, 0.001, 0.001, 0.000
5	BLYP	0.421	1.421	0.579	17.76	82.24	2.000, 1.999, 1.999, 1.999, **1.421**, 1.000, 1.000, 1.000, 1.000, **0.579**, 0.001, 0.001, 0.001, 0.000
	B3LYP	0.236	1.236	0.764	5.58	94.42	2.000, 1.999, 1.999, 1.999, 1.998, 1.997, **1.236**, 1.000, 1.000, 1.000, 1.000, **0.764**, 0.003, 0.002, 0.001, 0.001, 0.001, 0.000
6	BLYP	0.611	1.611	0.389	37.33	62.67	2.000, 1.999, 1.999, **1.611**, 1.000, 1.000, 1.000, 1.000, **0.389**, 0.001, 0.001, 0.000
	B3LYP	0.358	1.358	0.642	12.83	87.17	2.000, 1.999, 1.999, 1.999, 1.999, 1.999 1.997, **1.358**, 1.000, 1.000, 1.000, 1.000, **0.642**, 0.003, 0.001, 0.001, 0.001, 0.001, 0.001, 0.000
7	BLYP	0.566	1.566	0.434	32.05	67.95	2.000, 1.999, 1.999, 1.999, **1.566**, 1.000, 1.000, 1.000, 1.000, **0.434**, 0.001, 0.001, 0.001, 0.000
	B3LYP	0.425	1.425	0.575	18.06	81.93	2.000, 1.999, 1.999, 1.999, 1.999, 1.998 1.997, **1.425**, 1.000, 1.000, 1.000, 1.000, **0.575**, 0.003, 0.002, 0.001, 0.001, 0.001, 0.001, 0.000

It can be shown easily that $\langle S^2\rangle$ obtained from the weights of basic determinants (see ref 37, formula 4.1) will have an almost exact value within a given accuracy.

As seen in Figure 2, the natural orbitals (λ_1, μ_1) calculated at the B3LYP level for all systems appear to be bonding and antibonding combinations of one of the d orbitals of iron and the π^* orbital of nitrobenzene. The natural orbitals obtained at the BLYP level have the same shape. There is only one exception, compound **1**; its natural orbitals (λ_1, μ_1) predominantly consist of the d_{x2-y2} orbital of iron. In other words, there is no covalent chemical bonding and corresponding significant electron redistribution at the frontier orbitals in this system. The nature of its interaction is close to the physical-type adsorption. The shape of the active paired orbitals (Figure 3) arising from these natural orbitals is discussed below. Surprisingly, the a_1 orbitals for **1**−**4** are the same and represent the almost pure $d_{x^2-y^2}$ orbital of iron. However, the addition of a third OH group to the iron center alters the orbital responsible for the interaction. Consequently, the a_1 orbital for **5** is an almost pure d_{xz} orbital and for **6** and **7** has d_{z^2} character. The corresponding a_1^v orbitals for all systems are found to be the π^* orbital of nitrobenzene that is localized on the nitro group. Four singly occupied natural and paired orbitals for all systems (Table 3) appear to be the almost pure four other d orbitals of iron (not shown).

As was argued before,[42] the most convenient way for the expansion of the KS determinant is to express it in the basis of the a_r and a_r^v orbitals due to their localized character. In this basis Ψ_{KS} of the $S_z = 2$ state of $\{Fe(PhNO_2)\}^6$ (for both DFT functionals) can be written down as a linear combination of two restricted determinants

$$\Psi_{KS} = C^0|(\textit{inactive shells})a_1\alpha\, a_1\beta + C^1|(\textit{inactive shells})a_1\alpha\, a_1^v\beta\rangle = C^0D^0 + C^1D^1 \quad (1)$$

where expansion coefficients C are determined by the overlap $\langle a_1|b_1\rangle$. Determinants for each case can be expressed via specific a_r and a_r^v and singly occupied orbitals. For instance, for **1**−**3**

$$\Psi_{KS}(1) = C^0|(\textit{closed shells})(d_{z^2}\alpha d_{xy}\alpha d_{xz}\alpha d_{yz}\alpha)d_{x^2-y^2}\alpha d_{x^2-y^2}\beta\rangle + C^1|(\textit{closed shells})(d_{z^2}\alpha d_{xy}\alpha d_{xz}\alpha d_{yz}\alpha)d_{x^2-y^2}\alpha\pi^*\beta\rangle \quad (2)$$

In the same way, for **5** for example

$$\Psi_{KS}(1) = C^0|(\textit{closed shells})(d_{x^2-y^2}\alpha d_{xy}\alpha d_{yz}\alpha d_{z^2}\alpha)d_{xz}\alpha d_{xz}\beta\rangle + C^1|(\textit{closed shells})(d_{x^2-y^2}\alpha d_{xy}\alpha d_{yz}\alpha d_{z^2}\alpha)d_{xz}\alpha\pi^*\beta\rangle \quad (3)$$

and so on.

The obtained determinants can be assigned to the specific configurations. Indeed, D^0 corresponds to $[Fe^{+2}(d^6, S = 2) - PhNO_2(S = 0)]$ with π-type covalent bonding between specific d and π^* orbitals of iron and nitrobenzene. D^1 corresponds to the charge-transfer configuration $[Fe^{+3}(d^5, S = 5/2) - \{PhNO_2\}^-((\pi^*)^1, S = 1/2)]$ with antiferromagnetically coupled iron and -NO_2 centers. The last configuration represents oxidized Fe(III) and reduced nitrobenzene anion radical.

The actual weights of these configurations (Table 3) depend on many factors such as molecular environment, the angle between overlapping orbitals, the number of ligands next to iron, and obviously the nature of the DFT fuctional. As is expected,[32,39] the hybrid functionals (e.g., B3LYP) favor charge-transfer configurations. The somewhat lower population of the above configuration predicted by the BLYP functional is, in our opinion, less reliable.

The contribution of the covalent configuration for compounds **1**, **3**, and **4** appears to be predominant (83−99%) as predicted by both the B3LYP and the BLYP functionals. It clearly stands that in **1** the excess positive charge in the system effectively prevents the reduction of nitrobenzene. For the other two systems (**3** and **4**), the spatial arrangements of the interacting orbitals disfavor their effective overlap. The next extreme case is **5** where both functionals predict the predominance (84−95%)

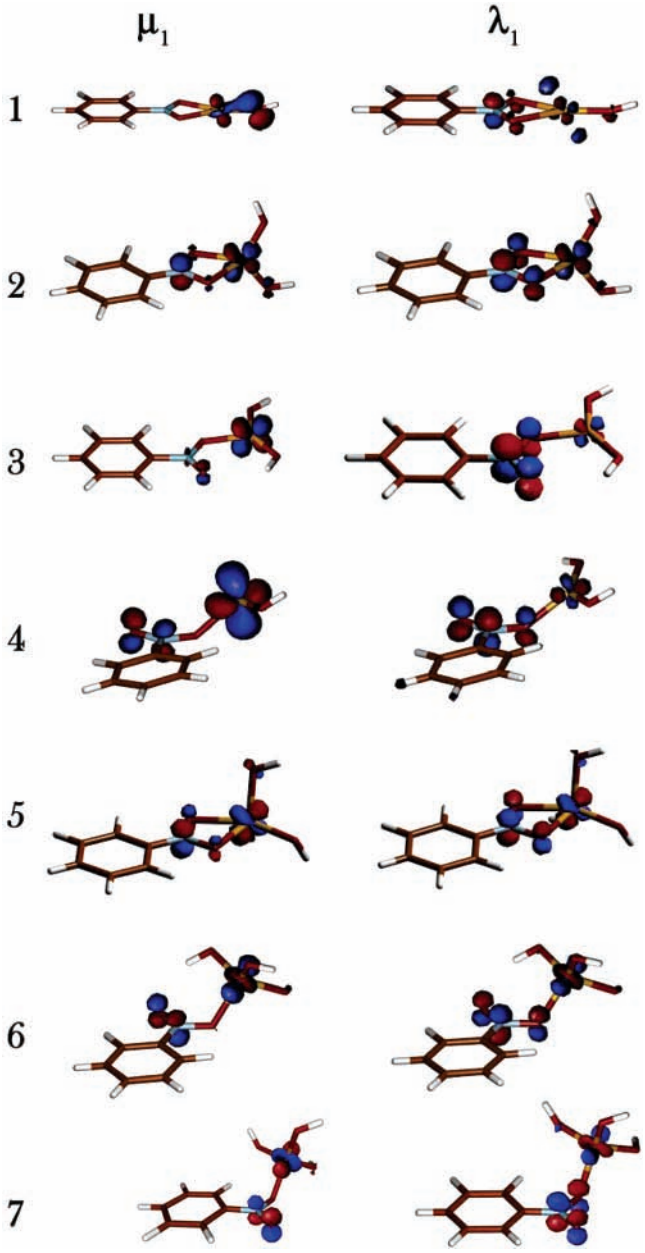

Figure 2. Active natural orbitals for **1**−**7** as obtained at the UB3LYP/6-311+G(d) level. Red (blue) color indicates higher (lower) conductance. The red and blue colors reflect positive and negative phases of the orbital.

of the charge-transfer configuration. Somewhere in between lie the rest of the compounds **2**, **6**, and **7** where two forms are in approximate balance with each other (48%, 37%, and 37% of the covalent form, respectively) as predicted by BLYP. In contrast, B3LYP reveals predominance (86%, 87%, and 85%, respectively) of the charge-transfer form. It is obvious that the excess charge promotes the nitrobenzene reduction in the system. Because different d orbitals of iron are responsible for interaction with nitrobenzene, this facilitates efficient electron transfer from the ferrous center for both the κ^2 symmetric and the κ^1 side-on/out-of-plane complexes.

Conclusions

In summary, our studies based on the UDFT approach provide insight into the electronic structure and bonding of the {Fe(PhNO$_2$)}^{6} unit using model nitrobenzene complexes with cationic, neutral, and anionic forms of the ferrous center.

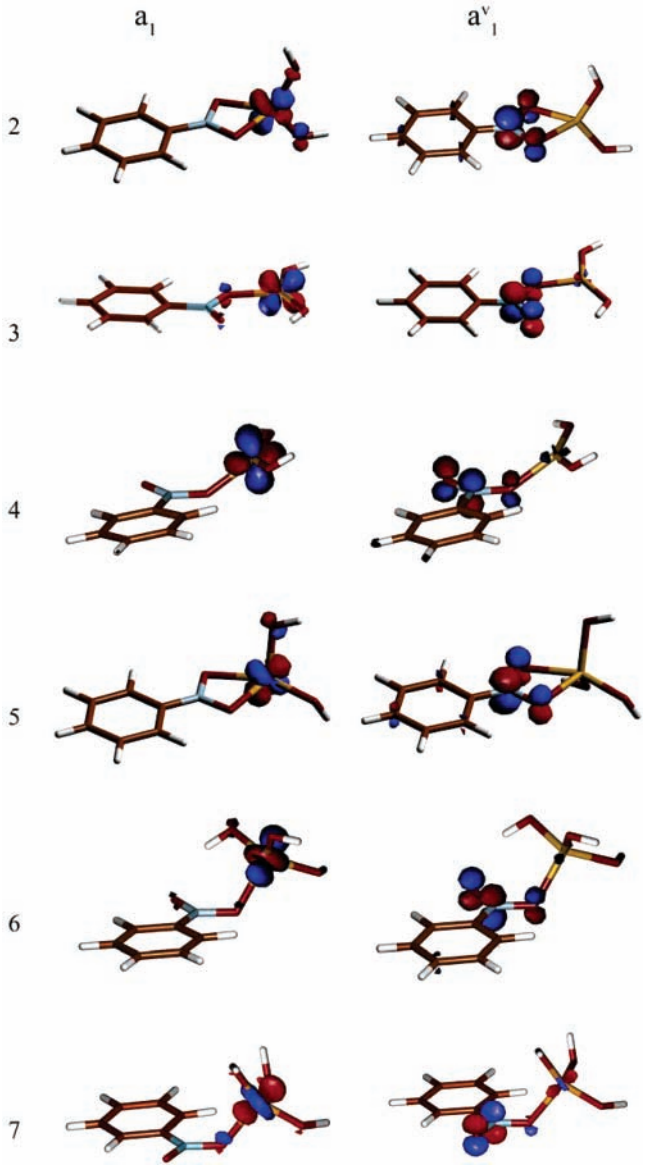

Figure 3. Paired a_1 and a_1^v orbitals for 2−7 as obtained from UB3LYP/6-311+G(d) level natural orbitals. The red and blue colors reflect positive and negative phases of the orbital.

The electronic structure of this unit can be expressed in terms of π-type covalent bonding [$Fe^{+2}(d^6, S = 2)$ − $PhNO_2(S = 0)$] and the charge-transfer configuration [$Fe^{+3}(d^5, S = 5/2)$ − $\{PhNO_2\}^-$ ($(\pi^*)^1$, $S = 1/2$)]. An excess negative charge on the ferrous center enhances the reduction of nitrobenzene (higher weight of charge-transfer configuration), whereas a positive charge effectively prevents this process (giving predominantly covalent bonding).

In complexes **2**−**4**, the $d_{x^2-y^2}$ orbital of iron is responsible for the bonding with nitrobenzene, favoring charge transfer only in the μ^2 symmetric complex **2**. In contrast with this, the d_{xz}, and d_{z^2} iron orbitals are utilized in **5**−**7** allowing effective reduction of nitrobenzene for all of them.

Acknowledgment. This work was supported by the U.S. Army Engineer Research and Development Center (ERDC) grant no. W912HZ-05-C-0051 and by the Army High Performance Computing Research Center (AHPCRC), Army Research Laboratory Cooperative Agreement no. DAAD19-01-2-0014, the content of which does not necessarily reflect the position or policy of the government, and no official endorsement should

be inferred. We thank the Mississippi Center for Supercomputing Research (MCSR) and AHPCRC for a generous allotment of computer time. We also thank Dr. Sergey Ph. Ruzankin for providing a program performing the S^2-expansion technique using regular Gaussian output.

References and Notes

(1) Zengel, H. G. *Chem.-Ing.-Tech.* **1983**, *55*, 962.
(2) Maltha, A.; Vanwermeskerken, S. C.; Brunet, B.; Ponec, V. *J. Mol. Catal.* **1994**, *93*, 305.
(3) Hofstetter, T. B.; Heijman, C. G.; Haderlein, S. B.; Holliger, C.; Schwarzenbach, R. P. *Environ. Sci. Technol.* **1999**, *33*, 1479.
(4) Scherer, M. M.; Johnson, M. K.; Westall, J. C.; Tratnyek, P. G. *Environ. Sci. Technol.* **2001**, *35*, 2804.
(5) Naka, D.; Kim, D.; Strathmann, T. J. *Environ. Sci. Technol.* **2006**, *40*, 3006.
(6) Weiss, W.; Ranke, W. *Prog. Surf. Sci.* **2002**, *70*, 1.
(7) Joyner, R.; Stockenhuber, M. *J. Phys. Chem. B* **1999**, *103*, 5963.
(8) Li, S.; Meitzner, G. D.; Iglesia, E. *J. Phys. Chem. B* **2001**, *105*, 5743.
(9) Elsner, M.; Schwarzenbach, R. P.; Haderlein, S. B. *Environ. Sci. Technol.* **2004**, *38*, 799.
(10) Devlin, J. F.; Klausen, J.; Schwarzenbach, R. P. *Environ. Sci. Technol.* **1998**, *32*, 1941.
(11) Hofstetter, T. B.; Schwarzenbach, R. P.; Haderlein, S. B. *Environ. Sci. Technol.* **2003**, *37*, 519.
(12) Klausen, J.; Haderlein, S. B.; Schwarzenbach, R. P. *Environ. Sci. Technol.* **1997**, *31*, 2642.
(13) Logue, B. A.; Westall, J. C. *Environ. Sci. Technol.* **2003**, *37*, 2356.
(14) Rodriguez, J. H.; Xia, Y. M.; Debrunner, P. G. *J. Am. Chem. Soc.* **1999**, *121*, 7846.
(15) Serres, R. G.; Grapperhaus, C. A.; Bothe, E.; Bill, E.; Weyhermuller, T.; Neese, F.; Wieghardt, K. *J. Am. Chem. Soc.* **2004**, *126*, 5138.
(16) Enemark, J. H.; Feltham, R. D. *Coord. Chem. Rev.* **1974**, *13*, 339.
(17) Hofstetter, T. B.; Neumann, A.; Schwarzenbach, R. P. *Environ. Sci. Technol.* **2006**, *40*, 235.
(18) Lee, J.; Kovalevsky, A. Y.; Novozhilova, I. V.; Bagley, K. A.; Coppens, P.; Richter-Addo, G. B. *J. Am. Chem. Soc.* **2004**, *126*, 7180.
(19) Thomas, J. L. C.; Bauschlicher, C. W.; Hall, M. B. *J. Phys. Chem. A* **1997**, *101*, 8530.
(20) Delley, B.; Wrinn, M.; Luthi, H. P. *J. Chem. Phys.* **1994**, *100*, 5785.
(21) Schultz, N. E.; Zhao, Y.; Truhlar, D. G. *J. Phys. Chem. A* **2005**, *109*, 11127.
(22) Gapeev, A.; Dunbar, R. C. *J. Am. Soc. Mass Spectrom.* **2002**, *13*, 477.
(23) Harvey, J. N. In *Principles and Applications of Density Functional Theory in Inorganic Chemistry I*; Springer-Verlag: Berlin, 2004; Vol. 112, p 151.
(24) Swart, M.; Groenhof, A. R.; Ehlers, A. W.; Lammertsma, K. *J. Phys. Chem. A* **2004**, *108*, 5479.
(25) Frisch, M. J.; Trucks, G. W.; Schlegel, H. B.; Scuseria, G. E.; Robb, M. A.; Cheeseman, J. R.; Montgomery, J. A., Jr.; Vreven, T.; Kudin, K. N.; Burant, J. C.; Millam, J. M.; Iyengar, S. S.; Tomasi, J.; Barone, V.; Mennucci, B.; Cossi, M.; Scalmani, G.; Rega, N.; Petersson, G. A.; Nakatsuji, H.; Hada, M.; Ehara, M.; Toyota, K.; Fukuda, R.; Hasegawa, J.; Ishida, M.; Nakajima, T.; Honda, Y.; Kitao, O.; Nakai, H.; Klene, M.; Li, X.; Knox, J. E.; Hratchian, H. P.; Cross, J. B.; Bakken, V.; Adamo, C.; Jaramillo, J.; Gomperts, R.; Stratmann, R. E.; Yazyev, O.; Austin, A. J.; Cammi, R.; Pomelli, C.; Ochterski, J. W.; Ayala, P. Y.; Morokuma, K.; Voth, G. A.; Salvador, P.; Dannenberg, J. J.; Zakrzewski, V. G.; Dapprich, S.; Daniels, A. D.; Strain, M. C.; Farkas, O.; Malick, D. K.; Rabuck, A. D.; Raghavachari, K.; Foresman, J. B.; Ortiz, J. V.; Cui, Q.; Baboul, A. G.; Clifford, S.; Cioslowski, J.; Stefanov, B. B.; Liu, G.; Liashenko, A.; Piskorz, P.; Komaromi, I.; Martin, R. L.; Fox, D. J.; Keith, T.; Al-Laham, M. A.; Peng, C. Y.; Nanayakkara, A.; Challacombe, M.; Gill, P. M. W.; Johnson, B.; Chen, W.; Wong, M. W.; Gonzalez, C.; Pople, J. A. *Gaussian 03*, revision C.02; Gaussian, Inc.: Wallingford, CT, 2004.
(26) Becke, A. D. *J. Chem. Phys.* **1993**, *98*, 1372.
(27) Lee, C. T.; Yang, W. T.; Parr, R. G. *Phys. Rev. B* **1988**, *37*, 785.
(28) Becke, A. D. *Phys. Rev. A* **1988**, *38*, 3098.
(29) Hay, P. J. *J. Chem. Phys.* **1977**, *66*, 4377.
(30) Wachters, A. J. *J. Chem. Phys.* **1970**, *52*, 1033.
(31) Raghavachari, K.; Trucks, G. W. *J. Chem. Phys.* **1989**, *91*, 1062.
(32) Schenk, G.; Pau, M. Y. M.; Solomon, E. I. *J. Am. Chem. Soc.* **2004**, *126*, 505.
(33) Glendening, E. D.; Badenhoop, J. K.; Reed, A. E.; Carpenter, J. E.; Bohmann, J. A.; Morales, C. M.; Weinhold. F. *NBO 5.0*; Theoretical Chemistry Institute, University of Wisconsin, Madison, 2001.
(34) Schaftenaar, G.; Noordik, J. H. *J. Comput.-Aided Mol. Des.* **2000**, *14*, 123.
(35) Löwdin, P. O. *J. Appl. Phys.* **1962**, *33*, 251.
(36) Amos, A. T.; Hall, G. G. *Proc. R. Soc. London, Ser. A* **1961**, *263*, 483.
(37) Zilberberg, I.; Ruzankin, S. P. *Chem. Phys. Lett.* **2004**, *394*, 165.
(38) Mikhalkova, A.; Gorb, L.; Leszczynski, J. Unpublished work.
(39) Zilberberg, I.; Ilchenko, M.; Isayev, O.; Gorb, L.; Leszczynski, J. *J. Phys. Chem. A* **2004**, *108*, 4878.
(40) Zilberberg, I.; Gora, R. W.; Zhidomirov, G. M.; Leszczynski, J. *J. Chem. Phys.* **2002**, *117*, 7153.
(41) Overhauser, A. W. *Phys. Rev.* **1962**, *128*, 1437.
(42) Zilberberg, I.; Ruzankin, S. P.; Malykhin, S.; Zhidomirov, G. M. *Chem. Phys. Lett.* **2004**, *394*, 392.